

N93-30874

Evaluation of Some Scale Effects in the Response and Failure of Composite Beams

Karen E. Jackson
U.S. Army Aerostructures Directorate, AVSCOM
NASA Langley Research Center

John Morton
Virginia Polytechnic Institute and State University
Blacksburg, VA

SUMMARY

The feasibility of using scale model testing for predicting full-scale behavior of composite beams loaded in tension and flexure was investigated. Classical laws of similitude were applied to fabricate and test replica model beams to identify scaling effects in the load response, strength, and mode of failure. Experiments were conducted using graphite-epoxy composite beams having different laminate stacking sequences and a range of scaled sizes. Results indicated that the elastic response of scaled composite beams was independent of specimen size. However, a significant scale effect in strength was observed. In addition, a transition in failure mode was observed among scaled beams of certain laminate stacking sequences. Weibull statistical and fracture mechanics based models were applied to predict the strength scale effect since standard failure criteria cannot account for the influence of absolute specimen size on failure.

INTRODUCTION

The high specific strength and stiffness characteristics of composite materials have led to their application in the development of advanced, weight-efficient military and commercial aircraft. Government, industry, and universities are currently working in cooperation on a research program designed to encourage the increased use of composite materials. The objective of this program, the Advanced Composites Technology (ACT) Program sponsored by the National Aeronautics and Space Administration (NASA), is to develop and demonstrate the technology base needed to ensure the cost effective use of advanced composite materials in primary structures of future aircraft [1]. In the absence of the broad design base available for metal structures, composite prototypes must be fabricated and tested as part of design evaluation. Such testing, especially if it involves destruction of the composite test article, is expensive and time consuming. Consequently, there is a growing interest in the use of structural scale model testing and the application of the principles of dimensional analysis to the testing and evaluation of fiber composite components. These principles have long played an important role in aerodynamic design and are being applied increasingly to complex structural problems. Currently, research efforts are in progress to study scaling effects in the fundamental behavior of composite coupons. Later this research will be applied to construct scale models of innovative fuselage concepts using composite materials through the ACT program. It is essential, however, to understand the limitations involved in testing scale model structures to ensure that the results obtained from sub-scale specimens provide valid predictions of prototype behavior.

In this paper, the results obtained from two investigations which were conducted to examine scaling effects in the response and failure of graphite-epoxy composite beams will be discussed. In the first study, Kellas and Morton [2] performed tensile tests on replica model beams having four different laminate stacking sequences and four different scaled sizes (1/4, 1/2, 3/4, and full-scale). The laminates were scaled on a ply level and were chosen

to highlight individual and interacting failure modes. In the second study, a series of tests were conducted by Jackson [3] to investigate the large deflection, flexural response of composite beams. Scale model beams ranging in size from 1/6 to full-scale were tested statically under an eccentric axial compressive load until failure. The loading configuration for the flexural tests is shown schematically in Figure 1. Four laminate stacking sequences including unidirectional, angle ply, cross ply, and quasi-isotropic were tested to examine a diversity of composite response and failure modes. For both the tensile and flexural tests, comparisons of elastic response, stiffness, ultimate strength and mode of failure between the prototype and scale model beams are made for each laminate type. Correlation of the test results will determine whether full-scale behavior can be predicted from scale model testing and indicate the limitations of applicability of scale model testing for composite structures.

BACKGROUND INFORMATION

The problem of designing and building a scale model structure constructed of advanced, fiber-reinforced composite materials is challenging due to the complexity of the material. In general, the construction of a scaled composite component may be examined on two levels. The most fundamental approach is to scale the constituent materials, the fiber and matrix. This approach is similar to the technique used to fabricate reinforced concrete model structures in which the reinforcing bars and aggregate size are scaled [4-7]. For a typical graphite-epoxy composite material system, scaling of the microstructure on this level would involve scaling of the fiber geometry and spacing within the matrix. Fiber volume fractions should be the same for both model and prototype systems. However, for most structural problems, this degree of scaling becomes impractical and infeasible.

The second approach is to scale the composite laminate on a macroscopic level by assuming that the individual lamina properties are smeared, i.e., the heterogeneous nature of the material is ignored on the microscopic level and the laminate is treated as a homogeneous, orthotropic sheet. Thus, in-plane and bending stiffnesses of the composite component are scaled by adjusting the number and location of plies within the laminate stacking sequence. This approach is practical when macroscopic structural aspects of the problem are more significant than material considerations for achieving scaled response. For example, to build a scale model of a stiffened panel, construction details such as stiffener geometry and spacing may influence the response to a higher degree than perhaps a minor irregularity in the microstructure of a single ply in the laminated panel. Thus, each level of structural complexity has its own unique set of scaling difficulties and special concerns.

In addition, it is necessary to understand how changes in the microstructure, including the initiation and growth of damage, accumulate in the material and affect the overall structural response at various dimensional scales. Haritos, et. al. [8] have introduced the term "mesomechanics" to describe the area of research which bridges the microstructure studies of fiber reinforced composites with structural mechanics theories. Unfortunately, little research has been published on this topic. Test data obtained in the laboratory on small coupon-type specimens are routinely assumed to be valid for full-scale structures with no regard for possible distortions due to size or scale. This assumption is made even though a size effect in failure behavior of metallic structures has been well documented [9-12].

Previous research on testing of scale model composite structures is limited. However, the available data generally fall into two categories. First is the application of scale model testing to large, complex structures. A few examples of research of this type include (1) construction and testing of a one-half scale helicopter fuselage sub-floor made from graphite-epoxy to investigate the nonlinear load-deflection behavior by Gustafson, et. al. [13], (2) development of a flexible wing model using a hybrid of E-glass and graphite-epoxy for wind tunnel testing by McCullers and Naberhaus [14], and (3) fabrication of a scale model of the Filament Wound Case (FWC) of the solid rocket motor of the space shuttle by Verderaime [15]. Each of these studies identified specific problems associated with fabricating and testing scale model structures using composite materials.

The second category of research which has been reported on scaling effects in composites concerns the influence of specimen size on failure. Often the term "scale effect" does not refer to replica model testing, but is used to describe the influence of varying certain geometrical parameters on the structural response. For example, Fairfull [16] studied scaling effects in the energy absorption behavior of axially crushed composite tubes. He varied the thickness-to-diameter (t/d) ratio of the tube while leaving the length unchanged. Even though the length had little effect on the mean crush load, it is often difficult to quantify the scale effect in failure response from geometrically distorted models. Recently, tests have been conducted to examine scaling effects in the impact response and failure of composite beams by Morton [17], and composite plates by Qian, et al, [18]. Results from these tests indicate that classical scaling laws apply for elastic dynamic response, but a size effect was observed as the beams became damaged under greater impact loads. In general, standard failure criteria used for composite strength analysis such as maximum stress, maximum strain, and tensor polynomial, cannot predict the strength scale effect. Statistical methods based on Weibull distributions [19-22], and fracture mechanics based theories [12,23] have been used to analyze the strength scale effect since they incorporate some measure of the absolute specimen size. The scaling studies performed on composite beams loaded in tension and flexure are significant because they bridge the gap between detailed microstructural studies on a material level and the testing of large, complicated structures on a macroscopic level.

CONCEPTS OF SIMILITUDE

The non-dimensional parameters which form the scaling law *for a given phenomenon* may be derived either from the governing equations and boundary conditions, or from the Pi Theorem. Both techniques are described and the advantages and disadvantages of each are discussed by Baker, et al. [24]. The Pi Theorem is the more general method of the two and consists of identifying the important physical variables relevant to the problem under consideration. Each variable is represented dimensionally in terms of a fundamental set of units, typically either the Force-Length-Time (F-L-T) system or the Mass-Length-Time (M-L-T) system. The law of dimensional homogeneity and the Pi Theorem are used in conjunction to derive the independent dimensionless products, or Pi terms. The Pi terms are not unique and may be multiplied together to form new combinations which are equally acceptable.

In the development of a scale model experiment, attempts are made to ensure that the Pi terms are identical for both the model and the prototype. In general, this may or may not be possible given the constraints of the problem. Scaling conflicts arise when Pi terms are not satisfied or when two Pi terms cannot be satisfied simultaneously. Typically, the geometric scale factor, λ (defined as the ratio of the model to the full-scale dimension), is chosen for the experiment. The scale factors for all other variables are then derived in terms of the geometric scale factor from the Pi terms and other conditions set by the experiment. When the constants of proportionality between variables used to describe the problem are known, then results from model tests can be "scaled up" to predict prototype response.

Various types of similarity may be defined between a model and prototype system including geometric, kinematic, dynamic (kinetic), and constitutive similarity. A model is said to be geometrically similar to its prototype if the dimensions have been scaled by the same factor. Thus, geometric similarity is ensured by fabricating beams with scaled lengths, widths, and thicknesses. In addition, for the flexural tests, the boundary conditions are scaled by applying a constant geometric scale factor to the hinge supports which provide the offset for the axial load. Kinematic similarity has been defined by Langhaar [25] as follows: "The motions of two systems are similar if homologous particles lie at homologous points at homologous times." Thus, kinematic similarity implies a relationship between the motions of two systems and is defined by the scale factors for position, time, velocity,

frequency, and acceleration between the model and prototype. Dynamic similarity between two systems exists if homologous parts of the systems experience homologous forces. If kinematic similarity exists for systems which have similar mass distributions, then dynamic similarity is easily inferred from Newton's Second Law. Since, in the present investigations, both the tensile and flexural tests were conducted under quasi-static conditions, kinematic and dynamic similarity were enforced by scaling the applied loads and boundary conditions.

Constitutive similarity is defined as homologous stress-strain behavior between the model and prototype systems in the loading range of interest. For laminated composite materials, constitutive similarity requires that the in-plane stiffnesses (A_{ij}) and bending stiffnesses (D_{ij}) of the model and prototype scale as λ and λ^3 , respectively. If the same prepreg material system is used to fabricate the laminated composite specimens, then density scales as unity. Geometrically scaled specimens are constructed by machining the length and width dimensions by the geometric scale factor, λ . The thickness dimension can be scaled by increasing the number of layers at each angular ply orientation within the laminate stacking sequence by the appropriate amount. This technique is often referred to as ply level scaling. Alternatively, the thickness dimension may be scaled on a sub-laminate level by increasing the number of ply groups within the laminate stacking sequence. For example, using ply level scaling, an eight ply, symmetric quasi-isotropic laminate $[0/90/\pm 45]_S$ may be scaled up by a factor of two to yield $[0_2/90_2/+45_2/-45_2]_S$. The same laminate would scale as $[(0/90/\pm 45)_2]_S$ using the sub-laminate approach. For this example, the in-plane stiffness of the one-half scale model and full-scale prototype is properly scaled using both techniques; however, the bending stiffness of the sub-laminate scaled specimen is distorted. The beam specimens which were fabricated for the tensile and flexural experiments were scaled on a ply level and were machined to the appropriate length and width dimensions for geometric similarity. Thus, modulus, cross-sectional area, and moment of inertia were properly scaled to achieve laminate scaling on a macroscopic level and to ensure constitutive similarity.

Scaling conflicts arise when time-dependent material properties are introduced into a dimensional analysis. Morton [17] has discussed the effect of rate-sensitive material behavior on constitutive similarity. If the same material is used to fabricate both the model and the prototype, then the strain rate parameter will be improperly scaled. This scaling distortion causes the model to experience greater strain rates than the prototype. For high strain rates, this result could cause brittle behavior in the model while the prototype exhibits ductile behavior at corresponding times during the loading. However, based on the findings from his investigation, Morton [17] concluded that rate effects were insignificant for the composite material system and laminates that he tested, but noted that these effects may become important for matrix-dominated laminates.

Elementary approaches to scaling indicate that under scaled loading conditions the stress state in the model is identical to that in the prototype, i.e., stress scales as unity. Ideally, then, failure should occur at the same stress and strain levels for both the model and full-scale specimens. However, deviations from this elementary approach to strength scaling are commonly observed. Typically, scale models predict higher failure loads than full-scale prototypes when the data are "scaled up" for comparison. One explanation for this size effect in strength is based on the principles of linear elastic fracture mechanics. A scaling conflict for stress is introduced when the critical stress intensity factor, K_Q , is included in a dimensional analysis [2,3]. Rather than a maximum stress or strain at failure, a critical stress intensity factor is defined as the parameter which governs the onset of unstable crack growth. Since composite materials often exhibit brittle fracture, it is reasonable to include a variable such as the critical stress intensity factor to model the failure behavior. The critical stress intensity factor, K_Q , is generally assumed to be a material property which is independent of loading conditions, initial crack geometry and size, or any other parameter. As such, K_Q should have the same value for both the model and the prototype. However, a dimensional analysis including K_Q as a variable requires that K_Q

be scaled in proportion to $\lambda^{1/2}$. Since this condition is violated when the geometric scale factor is λ , the stress at initiation of unstable crack propagation scales as $\lambda^{-1/2}$. Thus, the stress required to propagate a crack in a linear elastic model will be greater by a factor of $\lambda^{-1/2}$ than the stress needed to propagate a crack in a geometrically and constitutively similar prototype. As an example, the stress for crack propagation in a 1/4 scale structural model will be twice the value required for the full-scale structure. Consequently, the model will appear twice as strong.

EXPERIMENTAL PROGRAM

Two experimental investigations were conducted to examine scaling effects in the response and failure of composite beams loaded in tension and flexure. In both studies, scale model beams were constructed of Magnamite AS4/3502 graphite-epoxy composite material by adjusting the number of plies for each angular orientation in the laminate stacking sequence. Ply level scaling in this manner should produce composite beams in which the in-plane and bending stiffnesses are properly scaled. For both the tensile and flexural tests, care was taken to ensure that boundary and loading conditions were scaled for each beam specimen.

Tensile Tests.- Four laminates and four scaled sizes were selected for tensile testing; full-scale, 3/4, 1/2, and 1/4. The four laminates were

| | |
|-------------|-------------------------|
| Laminate A: | $(\pm 30_n/90_{2n})_S$ |
| Laminate B: | $(\pm 45_n/0_n/90_n)_S$ |
| Laminate C: | $(90_n/0_n/90_n/0_n)_S$ |
| Laminate D: | $(\pm 45_n/\pm 45_n)_S$ |

with n equal to 4, 3, 2, and 1, respectively. These laminate stacking sequences were chosen to highlight individual and interacting failure modes. Beam specimen geometric details are given in Table 1. The grip length of each beam was scaled to provide similar end conditions during loading, as indicated in Table 1. Beam specimens were tested in a mechanical load test machine equipped with wedge type grips. The cross-head displacement of the testing machine was adjusted such that each specimen was tested at approximately the same strain rate. Load and cross-head displacement were recorded from output of the testing machine. Strain was measured from both a foil strain gage located at the center of the beam and an extensometer for each scaled beam specimen. More details of the experimental procedure are provided in Reference [2].

Flexural Tests.- Beams having unidirectional, angle ply, cross ply, and quasi-isotropic laminate stacking sequences were tested under an eccentric compressive load to examine unique composite response and failure behaviors in flexure. Eight different sizes of beams were tested including full-scale, 5/6, 3/4, 2/3, 1/2, 1/3, 1/4, and 1/6 scale. The dimensions and lay-ups of each of the scale model beams are listed in Table 2. Note that use of ply level scaling rendered it impossible to construct a 1/4 or 3/4 scale quasi-isotropic beam.

The basic loading configuration for the scaled beams is shown in the schematic drawing of Figure 1. Each beam specimen was gripped in a set of hinges which offset the axial load with a moderate eccentricity. A detailed drawing of the hinge and beam attachment is shown in Figure 2. Eight sets of hinges were constructed (one for each of the eight scale factors) to ensure that the boundary and loading conditions were properly scaled. For each hinge, the eccentricity, grip length, and total distance from the center of the pin to the unsupported or free portion of the beam were scaled.

The hinges were pinned to the platens of a standard load test machine which applied the compressive vertical load. The hinged-pinned connection allowed the beam to undergo large rotations during deformation. Beam specimens were loaded in this manner until

catastrophic failure, defined as loss of load-carrying capability. The beam-column loading configuration was chosen, in part, because failures occur in a global fashion at the center of the beam where the maximum bending moment occurs. Thus, failures are not introduced by local effects at the grip supports. Although the beam was loaded as a beam-column, the bending strains were several orders of magnitude greater than those due to the axial compressive load. Therefore, the beam was nearly in a state of pure bending.

The vertical applied load was measured from a load platform located at the base of the bottom hinge support which was attached to the lower platen of the test machine. The distance traveled by the platens of the load test machine during a test is defined as the end displacement for that test. End displacement was measured from a string potentiometer displacement transducer. Strain measurements were recorded from back-to-back gages applied at the midpoint of the beams. Additional information on the experimental procedure used for the flexural tests is reported in Reference [3].

RESULTS

Scaling Effects in Initial Stiffness and Response

Tensile Tests.- A summary of the longitudinal initial stiffness (modulus) values as determined from extensometer and central strain gage data are listed in Table 3 for each of the scaled beams tested under tensile loading conditions. The stiffness values are valid for small strains only (0.2%, 0.5%, 0.5%, and 0.35% strain for Laminates A, B, C, and D, respectively). In addition, the initial stiffnesses of the beams, as determined from lamination theory, are included in Table 3 for comparison with the experimental data. The material properties of the AS4/3502 composite material used in the lamination theory predictions are

$$E_1 = 19.85 \text{ Msi}$$

$$E_2 = 1.43 \text{ Msi}$$

$$G_{12} = 0.70 \text{ Msi}$$

$$\nu_{12} = 0.293$$

These data were determined by Sensmeier [26] from material characterization tests on the AS4/3502 material system. A correction factor of 0.87 was applied to the shear modulus, G_{12} , which was originally reported as 0.82 Msi to account for the non-uniformity of the shear stress field in the test method used [27]. The data presented in Table 3 show that the stiffness measurements derived from the central strain gage and from the extensometer are fairly consistent, and that the stiffness values calculated from lamination theory are slightly higher than the experimentally determined values for each of the four laminates. The data listed in Table 3 indicate that all specimen sizes of a particular laminate stacking sequence have approximately the same initial stiffness or modulus. Thus, no scale effect is seen in the initial stiffness of the composite beams loaded in tension.

Flexural Tests.- The effective bending stiffness of each of the scale model beams tested under flexural loading was determined empirically using a technique described in Reference [3]. The bending stiffnesses were calculated from the load versus end displacement plots in the linear elastic, small deflection response region and were used to investigate scaling effects in the elastic response. In Figure 3, the bending stiffness values for the scale model beams were multiplied by the appropriate factor, normalized by the full-scale value, and plotted versus scale factor for the unidirectional, angle ply, cross ply, and quasi-isotropic laminates. Any significant deviation from the straight line drawn at 1.0 in Figure 3 may be interpreted as a scale effect. Results for the unidirectional, cross ply, and quasi-isotropic beams show deviations of less than 10% from scaled response. This variation can be explained by minor differences in thicknesses of the cured beams and experimental

error. However, the angle ply laminates exhibit a large scale effect in the bending stiffness response. The smaller beams are significantly stiffer than the full-scale beam to the extent that the 1/6 scale beam response is 1.5 times stiffer than the prototype response. This effect may be attributed to the presence of matrix cracks in the larger scale model beams which are not found in the smaller beams. The cracks may be induced from curing and fabrication stresses caused by blocking large numbers of plies of the same orientation together, as required to fabricate the scaled beams.

Based on the normalized load versus end displacement data reported in Reference 3, no deviations from scaled response were observed for the unidirectional and cross ply laminates, even under severe rotations and deformations. However, the angle ply and quasi-isotropic laminates deviated from scaled response as the deflections became large due to damage events which altered the beam stiffness. The effect was especially dramatic for the angle ply laminates which contain no 0° plies. In general, the degree of success in achieving scaled response is highly dependent on the laminate stacking sequence and, particularly, is a function of the number of 0° plies in the laminate.

Scaling Effects in Strength

Tensile Tests.- A summary of the tensile strength results is given in Table 4 including the failure stress and strain values and the normalized failure stress and strain values. Tensile failure stress, or strength, is defined as the maximum load divided by the measured cross sectional area of the beam specimen. Likewise, failure strain is the maximum recorded displacement divided by the extensometer gage length. The data from Table 4 indicate that tensile strength depends on specimen size. For all four lay-ups, the tensile strength decreases with increasing specimen size. However, the amount of strength degradation depends on the percentage of 0° plies in the given stacking sequence. In general, laminates with a high percentage of 0° plies exhibit a lower strength scale effect. For example, an 83% increase in strength was observed in 1/4 scale specimens of the matrix dominated Laminate A as compared to the full-scale specimens. In contrast, the average strength of the 1/4 scale specimens of the fiber dominated Laminate C was only 7% higher than the average strength of the full-scale specimens. This trend is depicted in Figure 4 which is a plot of the normalized strength versus scaled size.

The failure strains were also affected by specimen size, as indicated by the data listed in Table 4. The sensitivity of the size effect was determined by the laminate stacking sequence. For Laminates A, C, and D, the failure strains tended to increase with decreasing specimen size. However, an opposite effect was observed for Laminate B. Generally, the failure strains were found to depend on the method of measurement with noticeable differences between the gage readings and the extensometer data. Strain gages were often detached from the specimens prior to final failure and did not provide a true measure of the failure strain. Due to these difficulties, a failure analysis based on stress was considered more suitable for predicting the strength scale effect.

Flexural Tests.- A significant scale effect in strength was also observed for the four laminate types tested under flexural loading to failure. The loads, end displacements, and strains at failure increased as the size of the beams decreased from full-scale to 1/6 scale. To illustrate the magnitude of the strength scale effect, the failure loads for each of the scale model beams were multiplied by the appropriate scale factor ($1/\lambda^2$), normalized by the full-scale value, and plotted as a function of scale factor in Figure 5. If no scaling effects in strength were present, then all of the data would fall on the line drawn at 1.0. The plot indicates that a scale effect is evident even between the full and 5/6 scale beams. The effect increases as the size of the beams decreases. The cross ply laminate family exhibits the largest scale effect in strength among the laminates tested. The unidirectional laminates appear to be the least sensitive to the size effect in strength; although the effect is still observed.

Scaling Effects in Failure Mechanisms

Tensile Tests.- Final failure modes are shown in Figures 6-9 for Laminates A-D, respectively. The modes of failure for the fiber dominated laminates (B and C) were dependent on specimen size. In contrast to the strength behavior, the laminates containing the largest number of 0° plies were more sensitive to failure mode related scale effects than laminates having little or no 0° plies. For example, specimens of Laminate C which contained 50% 0° plies showed little variation in tensile strength with size. However, the mode of failure, as shown in Figure 8, changed from a clean fracture in the 1/4 scale beam to a brush-like fracture in the full-scale beam. Conversely, specimens of Laminate A and D which contained no 0° plies and exhibited a large strength-related size dependency, showed no apparent differences in failure mode related to specimen size.

For Laminate A, the smaller scale beams showed more delamination between the -30° and 90° plies at failure than the larger scale beams. However, in general, the overall mode of final failure was similar for all four sizes, as indicated in Figure 6. In the case of Laminate B, a transition in mode of failure was observed with increasing specimen size. Figure 7 shows that a localized type of fracture occurred in the small size beams whereas the larger beams showed an extensive fracture. Furthermore, small specimens exhibited a delamination in the 0°/90° interface as opposed to delamination between all interfaces in the larger sizes. Modes of final failure for Laminate C are shown in Figure 8. This family of specimens displayed the most pronounced transition in mode of final failure which changed from a clean, localized fracture in the small specimens to an extensive fracture occupying the whole gage length in the larger specimens. For matrix-dominated Laminate D, all four specimen sizes shared a very similar final failure mode, as shown in Figure 9, which was a localized $\pm 45^\circ$ shear fracture with minor delamination between the $\pm 45^\circ$ interfaces.

Flexural Tests.- Photographs of a complete set of failed beams are shown in Figures 10-13 for the unidirectional, angle ply, cross ply, and quasi-isotropic laminate families, respectively. No size-related differences in failure mechanism were observed for the unidirectional beams, shown in Figure 10, which failed by fiber fracture and longitudinal splitting. Since the maximum bending moment occurs in the center of the beam, final fracture of the fibers in the central region resulted in catastrophic beam failure. Likewise, the angle ply laminates showed no size dependency in mode of final failure. Figure 11 indicates that all specimen sizes failed by transverse matrix cracking along the 45° fiber direction. No fiber fractures were observed. Only the cross ply beams exhibited a size dependency in mode of failure, as shown in Figure 12. A transition in failure mechanism occurred between the 1/2 and 1/3 scale model beams in which the small size beams contained fiber fractures in the outer 0° plies and numerous transverse matrix cracks in the 90° core layer. However, no fiber fractures were observed for the larger size beams and a delamination between the 0° and 90° layers developed along the entire gage length. The quasi-isotropic beams failed through a combination of matrix cracking, delamination, and some fiber fractures, as shown in Figure 13. Although the smaller size beams appear to have sustained more damage than the larger beams, the mode of failure is similar for each size of beam.

DISCUSSION OF RESULTS

It was observed that initial stiffness and linear elastic, small-deflection response scale for the composite beams loaded in tension and flexure. This result implies that the fabrication technique used to construct the scale model composite beams provided constitutive similarity, and that the loading and boundary conditions were properly scaled to ensure scaled elastic response. A noted exception was the increase in bending stiffness with decreasing beam size exhibited by the angle ply laminates loaded in flexure. This behavior may be explained by the presence of damage in the larger size virgin specimens. Although evaluation techniques were not used to determine the damage state of the pre-tested beam

specimens for the flexural tests, evidence of matrix cracking in virgin specimens was detected in the tensile coupons of Laminate D. Figure 14 contains x-ray radiographs of virgin specimens of Laminate D which illustrate that the full-scale beam contained numerous transverse matrix cracks. The mechanism of crack formation and propagation is unknown at this time; however, crack density is higher in specimens containing large blocks of plies having the same orientation. Kellas and Morton [2] hypothesize that the observed cracks are driven by thermal residual stresses and may be triggered by specimen cutting, or by the generation of free edge stresses. For laminates containing some 0° plies, the effect of matrix damage in off-axis plies should not reduce the initial stiffness by a significant amount. However, transverse matrix cracks in angle ply laminates with no 0° plies could significantly reduce the stiffness and, thus, the elastic response of these laminates.

The presence of pre-existing damage in untested beam specimens may also contribute to the differences observed in the mode of failure among scaled sizes for certain laminates. As noted from the tensile test results, the fiber-dominated laminates B and C exhibited a transition in mode of final failure, whereas the matrix-dominated laminates A and D appeared to fail in a similar manner for each scaled size. For example, in Laminate A final failure is largely controlled by the load-bearing $\pm 30^\circ$ plies. The mode of failure was uniform for all four sizes because transverse matrix cracking along the $\pm 30^\circ$ fiber directions was a more likely failure mode than fiber breakage. The effect of transverse matrix cracking in the larger size beams was merely reflected in the reduced tensile strength. Similar behavior was seen for the matrix-dominated angle ply laminates tested under flexural loading. The progression of transverse matrix cracks along the $\pm 45^\circ$ fiber direction was the only failure mechanism available in these laminates. The effect of pre-existing cracks, if present, in the larger size specimens would be to reduce the ultimate strength. Thus, no transition in mode of failure was observed.

For fiber-dominated laminates loaded in tension, matrix cracks in the pretested beams served to decouple the plies which led to differences in failure mechanism between the smaller and larger scaled beams. Transverse matrix cracks in the small sizes of Laminate B, for example, developed as the beam was loaded and imposed a stress concentration in the neighboring 0° plies. As a result, a clean fracture in the 0° plies was observed. In the larger sizes of Laminate B, numerous transverse matrix cracks were already present in the virgin specimens. Consequently, under load, the larger size beams delaminated between the $0^\circ/90^\circ$ interface at a much lower applied stress than the smaller size beams. A similar transition in failure mechanism was seen in the response of the cross ply laminates under flexural loading. Fiber fractures were observed in the 0° plies of the 1/3 scale beams and smaller, while large delaminations were seen in the $0^\circ/90^\circ$ interface of the 1/2 scale beams and larger.

In general, it is believed that the size effect in strength which is observed on the macroscopic level is the result of microscopic damage which initiates within the laminate and develops in a certain manner under the applied load. The accumulation of damage and interaction of failure mechanisms eventually produce ultimate failure of the structure. Detailed investigations on the effect of test specimen size on failure need to be performed on a material level before the phenomenon can be thoroughly understood on the macroscopic level.

Analytical Predictions of the Strength Scale Effect

The increase in failure stress with decreasing specimen size in the tensile coupons, listed in Table 4, and the increase in failure load with decreasing specimen size in the flexure specimens, shown in Figure 5, demonstrate the magnitude of the strength scale effect. The observed differences in strength for replica model beams loaded under scaled conditions cannot be predicted based on standard failure criteria such as maximum stress, maximum strain, or tensor polynomial. Previous researchers have attempted to model the scale effect in strength of fiber-reinforced composite materials using either a statistical

approach [19-22] or a fracture mechanics model [12,23].

The application of statistical techniques for modeling the size effect in strength of brittle materials is based on the observation that these materials are flaw-sensitive. Since the presence of imperfections can be statistical in nature, it is reasonable to assume that larger specimens will exhibit lower strength simply because there is a higher probability that a strength-critical flaw is present in the greater volume of material. Weibull statistical theory has been applied in conjunction with a weakest link theory to develop a mathematical model for predicting the scale effect in strength. Bullock [20] found that the ratio of ultimate strengths between a geometrically similar model and prototype is given by

$$\frac{S_m^{\text{ult}}}{S_p^{\text{ult}}} = \left[\frac{V_p}{V_m} \right]^{1/\beta}$$

where the subscripts m and p refer to the model and prototype, respectively, and S^{ult} is the ultimate stress, V is the volume, and β is the Weibull shape parameter, sometimes called the flaw density parameter since it provides a measure of the scatter in the strength data. The flaw density parameter, β , is assumed to be a material constant. If β is determined empirically from two specimens of differing size, then the strength of geometrically similar scale models can be predicted.

Atkins and Caddell [12] used a fracture mechanics approach to derive a simple size-strength relationship for notched brittle materials. As discussed earlier in this paper, if the critical stress intensity factor is included in a dimensional analysis, the laws of similitude require that stress scale as $\lambda^{-1/2}$. Thus, the stress needed to propagate a crack in a full-scale prototype structure, σ_p , and the corresponding stress, σ_m , in a model structure are related by

$$\sigma_p = \sigma_m \sqrt{\lambda}$$

where λ is the geometric scale factor.

The Weibull statistical model and the fracture mechanics model were used to predict the strength of the full-scale laminates (A-D) for the tensile beam specimens and the results are listed in Table 5 along with the experimental data. For both models, the strength predictions were made by "scaling up" the 1/4 size strength data. The value of the flaw density parameter, β , was determined empirically based on strength data from the 1/4 and 1/2 scale sizes for each laminate type. Numerical values of β are listed in Table 5 and they ranged from 7.22 for Laminate A to 156.0 for Laminate C. The results presented in Table 5 indicate that the Weibull model provides the best strength prediction. However, this is expected since the flaw density parameter allows a curve to be fitted to the data.

The two strength prediction models were also applied to the flexure beam specimens. Figure 15 contains plots of the unidirectional, angle ply, cross ply, and quasi-isotropic normalized strength data with the Weibull statistical and the fracture mechanics based model predictions. In this case, the flaw density parameter was determined based on strength data from the 1/6 and full-scale size beams. As was observed for the tensile data, the Weibull model gives better strength predictions than the fracture mechanics model for the flexure data. The flaw density parameter varies depending on the laminate stacking sequence and must be determined empirically. The success of the Weibull model in predicting strength degradation depends heavily on the flaw density parameter which may be influenced by the initial state and size of the laminates used to derive it. For example, the flaw density parameter may be derived based on data from a 1/6 and a 1/4 scale model beam, neither of which contained pre-existing matrix cracks. If the full-scale laminate contained transverse matrix cracks due to fabrication stresses, then the Weibull model would overpredict the strength of the full-scale beam. Likewise, a transition in mode of final

failure between scaled sizes could reduce the effectiveness of a Weibull model if the transition is not somehow accounted for in the flaw density parameter.

Results of applying statistical and fracture mechanics based models for predicting the strength scale effect show that neither approach can explain the phenomenon in a satisfactory manner. Research by Crossman [28], Wang [29], and Laws [30] on the effects of transverse matrix cracking on the final fracture of cross ply laminates suggests that a model which incorporates both theories is needed. A statistical approach is used to determine which microflaws within the 90° core will coalesce to form a transverse matrix crack given a random distribution of flaws and flaw sizes. Once a crack has formed, fracture mechanics theories are applied to determine the stability of the crack under the given loading conditions. The progression of crack formation and stability are continually monitored until ultimate laminate failure. A model of this type has been used to predict the tensile failure of cross ply laminates in which the number of 90° plies was varied from 2 to 16 [30]. Although these laminates were not replica models since the number of 0° plies was not adjusted in the same proportion as the number of 90° plies, the success of the model indicates that it may be able to predict the stress required to initiate cracks in the transverse plies of scaled laminates of various stacking sequences.

CONCLUDING REMARKS

Two experimental investigations were conducted to examine scaling effects in the response and failure of graphite-epoxy composite beams loaded in tension and flexure. In both studies, the composite beams were fabricated using ply level scaling to ensure constitutive similarity. Both the tensile and flexural tests were performed under scaled loading and boundary conditions to determine the influence of specimen size on stiffness, elastic response, strength and failure mechanism. A variety of laminate stacking sequences were included in the experimental program to highlight individual and interacting failure modes. Major findings from these investigations are summarized in the following list.

1. In both the tensile and flexural tests, beam stiffnesses appeared to be independent of specimen size, especially in the loading range where small deflections, and small strains are valid and the material is linear elastic. Deviations from scaled response are observed when damage develops in the composite beams.
2. All specimens exhibited a scale effect in strength. Several factors influence the degree of sensitivity including the initial state of the laminate, and the laminate stacking sequence. For the tensile specimens, x-ray radiographs of the specimens prior to testing indicated that the larger size beams contained matrix cracks not seen in the smaller scale beams. These cracks may have initiated from fabrication or curing stresses. Once present, they serve as stress concentrations and contribute to the ultimate failure of the larger size beams. Also, the size effect in strength is influenced by the lay-up of the beam. Laminates with a higher percentage of 0° plies showed a smaller strength scale effect for tensile loaded specimens.
3. Transitions in the mode of final failure were evident for both tensile and flexural beams as the beam size increased. Again, this effect is dependent on lay-up. Scale model and prototype unidirectional, angle ply, and quasi-isotropic beams showed consistent failure mechanisms when tested to failure in flexure. However, cross ply beams showed a transition from matrix cracking and fiber breakage in the small scale beams, to delamination in the larger scaled beams. Some of the differences in failure mechanisms which occur as the size of the beam increases may be attributed to pre-existing matrix cracks.
4. The scale effect in strength was analyzed using a Weibull statistical approach and a fracture mechanics based model. These techniques have the capability of predicting a size effect in failure which standard composite failure criteria such as maximum stress, maximum strain, and tensor polynomial, cannot predict. The Weibull statistical model provided better correlation with the experimental results for both the tensile and flexural data than the fracture mechanics based model. However, the Weibull model requires additional empirical data and neither model is sensitive to the unique failure modes exhibited by composite laminates.

REFERENCES

1. Freeman, W. T.: "Innovation, Damage Tolerance, and Affordability NASA's New Thrust for Composites Research." presentation at the 1989 General Aviation Aircraft Meeting and Exposition, sponsored by the SAE, Wichita, Kansas, April 13, 1989.
2. Kellas, S.; and Morton, J.: "Strength Scaling in Fiber Composites." NASA CR 4335, October, 1990.
3. Jackson, K. E.: "Scaling Effects in the Static and Dynamic Response of Graphite-Epoxy Beam-Columns." NASA TM 102697, July, 1990.
4. Davies, I. L.: "Studies of the Response of Reinforced Concrete Structures to Short Duration Dynamic Loads." *Design For Dynamic Loading, The Use of Model Analysis*, G. S. T. Armer and F. K. Garas (eds.) London: Construction Press, 1982.
5. Murayama, Y.; and Noda, S.: "Study on Small Scale Model Tests for Reinforced Concrete Structures- Small Scale Model Tests by Using 3MM Diameter Deformed Re-bars." Kajima Institute of Construction Technology, Tokyo, Feb. 1983.
6. Pletta, D. H.; and Frederick, D.: "Model Analysis of a Skewed Rigid Frame Bridge and Slab." *Journal of the American Concrete Institute*, Vol. 26, No. 3, Nov. 1954, pp. 217-230.
7. Pletta, D. H.; and Frederick, D. : "Experimental Analysis." *Proceedings ASCE*, Vol. 79, No. 224, 1953.
8. Haritos, G. K.; Hager, J. W.; Amos, A. K.; Salkind, M. J.; and Wang, A. S. D.: "Mesomechanics: The Microstructure-Mechanics Connection." AIAA Paper 87-0726, A *Collection of Technical Papers Part 1*, 28th Structures, Structural Dynamics and Materials Conference, April 1987, pp. 812-818.
9. Booth, E.; Collier, D.; and Miles, J.: "Impact Scalability of Plated Steel Structures." *Structural Crashworthiness*. Jones and Wierzbicki, eds., London: Butterworths, 1983, pp. 136-174
10. Duffey, T. A.: "Scaling Laws For Fuel Capsules Subjected to Blast, Impact, and Thermal Loading." *Proceedings of the 1971 Intersociety Energy Conversion Engineering Conference*, Boston, Mass., August 1971, pp. 775-786.
11. Jones, N.: "Scaling of Inelastic Structures Loaded Dynamically." *Structural Impact and Crashworthiness*, Davies, ed., Vol. 1 Keynote Lectures, London: Elsevier Applied Science Publishers, 1984, pp. 46-71.
12. Atkins, A. G.; and Caddell, R. M.: "The Laws of Similitude and Crack Propagation." *International Journal of Mechanical Sciences*, Vol. 16, 1974, pp. 541-548.
13. Gustafson, A. J.; Ng, G. S.; and Singley, G. T.: "Impact Behavior of Fibrous Composites and Metal Substructures." USAAVRADCOM TR-82-D-31, 1982.
14. McCullers, L. A.; and Naberhaus, J. D.: "Automated Structural Design and Analysis of Advanced Composite Wing Models." *Computers and Structures*, Vol. 3, 1973, pp. 925-937.
15. Verderaiame, V. S.: "Scaling Phenomena of Graphite-Epoxy Wound Cases." *Proceedings of the Seventh Conference on Fibrous Composites in Structural Design*, AFWAL-TR-85-

3094, June 1985.

16. Fairfull, A. H.: "Scaling Effects in the Energy Absorption of Axially Crushed Composite Tubes." Ph.D. dissertation, University of Liverpool, 1986.
17. Morton, J.: "Scaling of Impact-Loaded Carbon-Fiber Composites." *AIAA Journal*, Vol. 26, No. 8, August 1988, pp. 989-994.
18. Qian, Y.; Swanson, S. R.; Nuismer, R. J.; and Bucinell, R. B.: "An Experimental Study of Scaling Rules for Impact Damage in Fiber Composites." *Journal of Composite Materials*, Vol. 24, No. 5, May 1990, pp. 559-570.
19. Zweben, C.: "The Effect of Stress Nonuniformity and Size on the Strength of Composite Materials." *Composites Technology Review*, Vol. 3, No. 1, 1981, pp. 23-26.
20. Bullock, R. E.: "Strength Ratios of Composite Materials in Flexure and Tension." *Journal of Composite Materials*, Vol. 8, April 1974, pp. 200-206.
21. Wang, A. S. D.; Tung, R. W.; and Sanders, B. A.: "Size Effect on Strength and Fatigue of a Short Fiber Composite Material." *Emerging Technologies in Aerospace Structures, Design, Structural Dynamics and Materials*, ASME, August 1980, pp. 37-52.
22. Chou, P. C.; and Croman, R.: "Scale Effect in Fatigue of Composite Materials." *Journal of Composite Materials*, Vol. 13, July 1979, pp. 178-194.
23. Carpinteri, A.; and Bocca, P.: "Transferability of Small Specimen Data to Full-Size Structural Components." *Composite Material Response: Constitutive Relations and Damage Mechanisms*, G. C. Sih, G. F. Smith, I. H. Marshall, and J.J. Wu (eds.) London: Elsevier Applied Science, 1987.
24. Baker, W. E.; Westine, P. S.; and Dodge, F. T.: *Similarity Methods in Engineering Dynamics*. Rochelle Park, N.J.: Hayden Book Company, 1973.
25. Langhaar, H. L.: *Dimensional Analysis and Theory of Models*. New York: John Wiley and Sons, Inc., 1951.
26. Sensmeier, M. D.; Griffin, O. H.; and Johnson, E. R.: "Static and Dynamic Large Deflection Flexural Response of Graphite-Epoxy Beams." NASA CR 4118, March 1988.
27. Morton, J.; Ho, H.; Tsai, M. Y.; and Farley, G. L.: "An Evaluation of the Iosipescu Specimen for Composite Materials Shear Properties Measurement." to be published in *Journal of Composite Materials*.
28. Crossman, F. W.; Warren, W. J.; and Wang, A. S. D.: "Influence of Ply Thickness on Damage Accumulation and Final Fracture." *Advances in Aerospace Structures, Materials, and Dynamics: A Symposium on Composites*, ASME Publication AD-06, 1983, pp. 215-226.
29. Wang, A.S.D.; Chou, P.C.; and Lei, S.C.: "A Stochastic Model for the Growth of Matrix Cracks in Composite Laminates." *Advances in Aerospace Structures, Materials, and Dynamics: A Symposium on Composites*, ASME Publication AD-06, 1983, pp. 7-16.
30. Laws, N.; and Dvorak, G.J.: "Progressive Transverse Cracking in Composite Laminates." *Journal of Composite Materials*, Vol. 22, October 1988, pp. 900-916.

TABLE 1.- Tensile specimen geometric details.

| | 1/4 SIZE | 2/4 SIZE | 3/4 SIZE | FULL SCALE |
|---|----------|----------|----------|------------|
| No. of plies | 8 | 16 | 24 | 32 |
| Average thickness in. x 10 ⁻³ | 44 | 88 | 133 | 176 |
| Nominal width in. | 0.5 | 1.0 | 1.5 | 2.0 |
| Nominal gage length / in. | 3.5 | 7.0 | 10.5 | 14.0 |
| Nominal gripped length / in. | 0.75 | 1.50 | 2.25 | 3.00 |
| No. of specimens | 22 | 10 | 12 | 10 |

TABLE 2.- Flexural beam specimen dimensions and lay-ups.

| Scale | Beam dimension | Uni-directional | Angle ply | Cross ply | Quasi-isotropic |
|-------|----------------|--------------------|--|---|--|
| 1/6 | 0.5" x 5.0" | [0] _{8T} | [45 ₂ / ⁻ 45 ₂] _s | [0 ₂ / ⁹⁰ 2] _s | [-45/0/45/90] _s |
| 1/4 | 0.75" x 7.5" | [0] _{12T} | [45 ₃ / ⁻ 45 ₃] _s | [0 ₃ / ⁹⁰ 3] _s | ----- |
| 1/3 | 1.0" x 10.0" | [0] _{16T} | [45 ₄ / ⁻ 45 ₄] _s | [0 ₄ / ⁹⁰ 4] _s | [-45 ₂ / ⁰ 2/45 ₂ / ⁹⁰ 2] _s |
| 1/2 | 1.5" x 15.0" | [0] _{24T} | [45 ₆ / ⁻ 45 ₆] _s | [0 ₆ / ⁹⁰ 6] _s | [-45 ₃ / ⁰ 3/45 ₃ / ⁹⁰ 3] _s |
| 2/3 | 2.0" x 20.0" | [0] _{32T} | [45 ₈ / ⁻ 45 ₈] _s | [0 ₈ / ⁹⁰ 8] _s | [-45 ₄ / ⁰ 4/45 ₄ / ⁹⁰ 4] _s |
| 3/4 | 2.25" x 22.5" | [0] _{36T} | [45 ₉ / ⁻ 45 ₉] _s | [0 ₉ / ⁹⁰ 9] _s | ----- |
| 5/6 | 2.5" x 25.0" | [0] _{40T} | [45 ₁₀ / ⁻ 45 ₁₀] _s | [0 ₁₀ / ⁹⁰ 10] _s | [-45 ₅ / ⁰ 5/45 ₅ / ⁹⁰ 5] _s |
| 6/6 | 3.0" x 30.0" | [0] _{48T} | [45 ₁₂ / ⁻ 45 ₁₂] _s | [0 ₁₂ / ⁹⁰ 12] _s | [-45 ₆ / ⁰ 6/45 ₆ / ⁹⁰ 6] _s |

TABLE 3.- Initial longitudinal stiffness (modulus) values from tensile tests. Values shown represent the average of six or more extensometer tests. Stiffness values are valid for small strains only: 0.2%, 0.5%, 0.5%, and 0.35% strain for Laminates A, B, C, and D, respectively.

INITIAL STIFFNESS (MODULUS), MSI

| SIZE n=1,2,3,4 | CENTRAL GAGES | EXTENSOMETER | LAMINATION THEORY |
|---|------------------|--------------|----------------------|
| LAMINATE A: $(\pm 30_n/90_{2n})_S$ | | | |
| 1/4 | 5.4 | 5.1 | 6.3 |
| 1/2 | 5.3 | 5.2 | 6.3 |
| 3/4 | 5.1 | 5.2 | 6.3 |
| Full | 5.0 | 6.1 | 6.3 |
| LAMINATE B: $(\pm 45_n/0_n/90_n)_S$ | | | |
| 1/4 | 7.0 | 6.8 | 7.7 |
| 1/2 | 6.8 | 6.8 | 7.7 |
| 3/4 | * | * | 7.7 |
| Full | 6.4 | 6.5 | 7.7 |
| LAMINATE C: $(90_n/0_n/90_n/0_n)_S$ | | | |
| 1/4 | 9.8 | 9.4 | 10.7 |
| 1/2 | 10.0 | 10.2 | 10.7 |
| 3/4 | * | * | 10.7 |
| Full | * | * | 10.7 |
| LAMINATE D: $(45_n/-45_n/45_n/-45_n)_S$ | | | |
| 1/4 | 2.4 | 2.2 | 2.5 |
| 1/2 | 2.5 | 2.4 | 2.5 |
| 3/4 | 2.4 | 2.4 | 2.5 |
| Full | 2.4 | 2.8 | 2.5 |

* - indicates insufficient data

TABLE 4.- Summary of the experimental strength and failure strain results from tensile tests: average values from six or more valid tests per condition.

| SIZE | TENSILE STRENGTH ksi | FAILURE STRAIN % | NORMALIZED STRENGTH | NORMALIZED STRAIN |
|---|-------------------------|---------------------|---------------------|-------------------|
| Lay-Up A (+30° _n /-30° _n /90° _{2n}) _s | | | | |
| 1/4 | 30.28 | 0.60 | 1.83 | 1.88 |
| 2/4 | 22.70 | 0.55 | 1.37 | 1.74 |
| 3/4 | 19.01 | 0.33 | 1.15 | 1.04 |
| full scale | 16.58 | 0.32 | 1.00 | 1.00 |
| Lay-Up B (+45° _n /-45° _n /0° _n /90° _n) _s | | | | |
| 1/4 | 80.78 | 1.20 | 1.39 | 0.82 |
| 2/4 | 72.35 | 1.18 | 1.24 | 0.81 |
| 3/4 | 61.97 | 1.42 | 1.06 | 0.97 |
| full scale | 58.34 | 1.47 | 1.00 | 1.00 |
| Lay-Up C (90° _n /0° _n /90° _n /0° _n) _s | | | | |
| 1/4 | 128.26 | 1.38 | 1.07 | 1.48 |
| 2/4 | 126.56 | 1.17 | 1.05 | 1.26 |
| 3/4 | 125.58 | 1.25 | 1.04 | 1.34 |
| full scale | 120.42 | 0.93 | 1.00 | 1.00 |
| Lay-Up D (+45° _n /-45° _n /+45° _n /-45° _n) _s | | | | |
| 1/4 | 19.63 | 1.05 | 1.56 | 2.49 |
| 2/4 | 17.08 | 0.96 | 1.36 | 2.29 |
| 3/4 | 14.96 | 0.74 | 1.19 | 1.77 |
| full scale | 12.56 | 0.42 | 1.00 | 1.00 |

TABLE 5.- Tensile strength predictions for full-scale Laminates A-D, based on Weibull statistical model and a fracture mechanics based model.

| LAMINATE TYPE | STRENGTH ksi | | |
|---------------|-----------------------|---------------------------|--------------------------|
| | EXPERIMENT FULL-SCALE | WEIBULL STATISTICAL MODEL | FRACTURE MECHANICS MODEL |
| A | 16.6 | 17.0 ($\beta=7.22$) | 15.1 |
| B | 58.3 | 64.7 ($\beta=18.8$) | 40.4 |
| C | 120.4 | 124.9 ($\beta=156.0$) | 64.1 |
| D | 12.6 | 14.8 ($\beta=14.87$) | 9.8 |

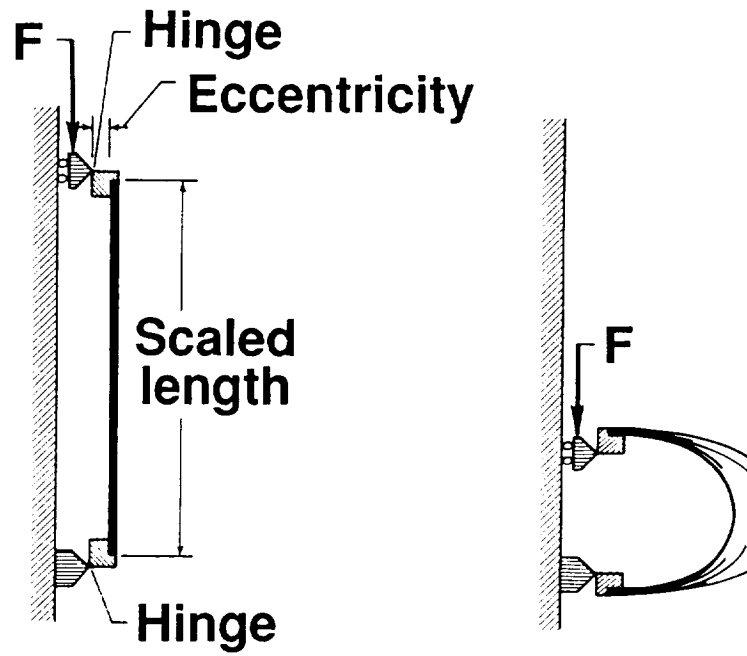


FIGURE 1. Schematic drawing of the flexural test configuration.

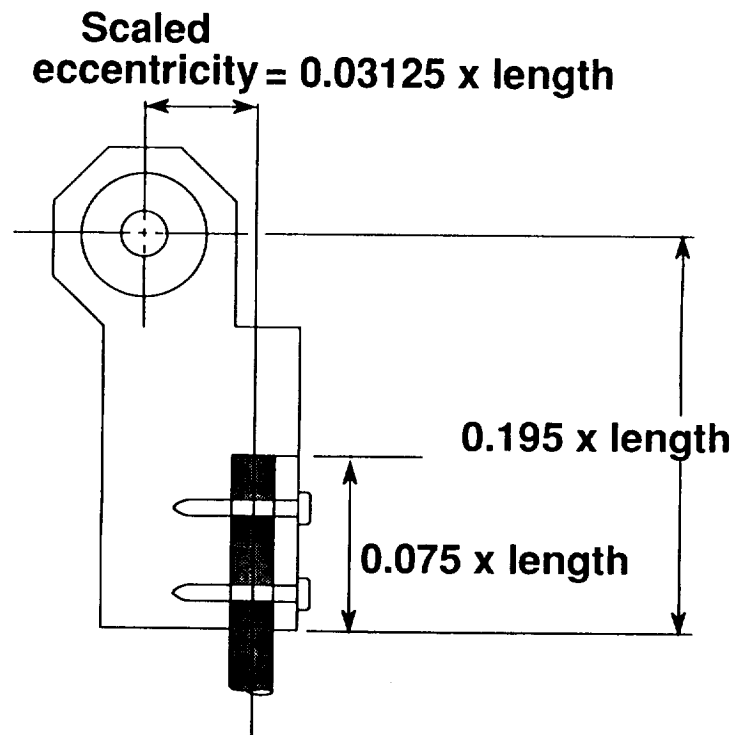


FIGURE 2. Detailed drawing of the hinge-beam attachment.

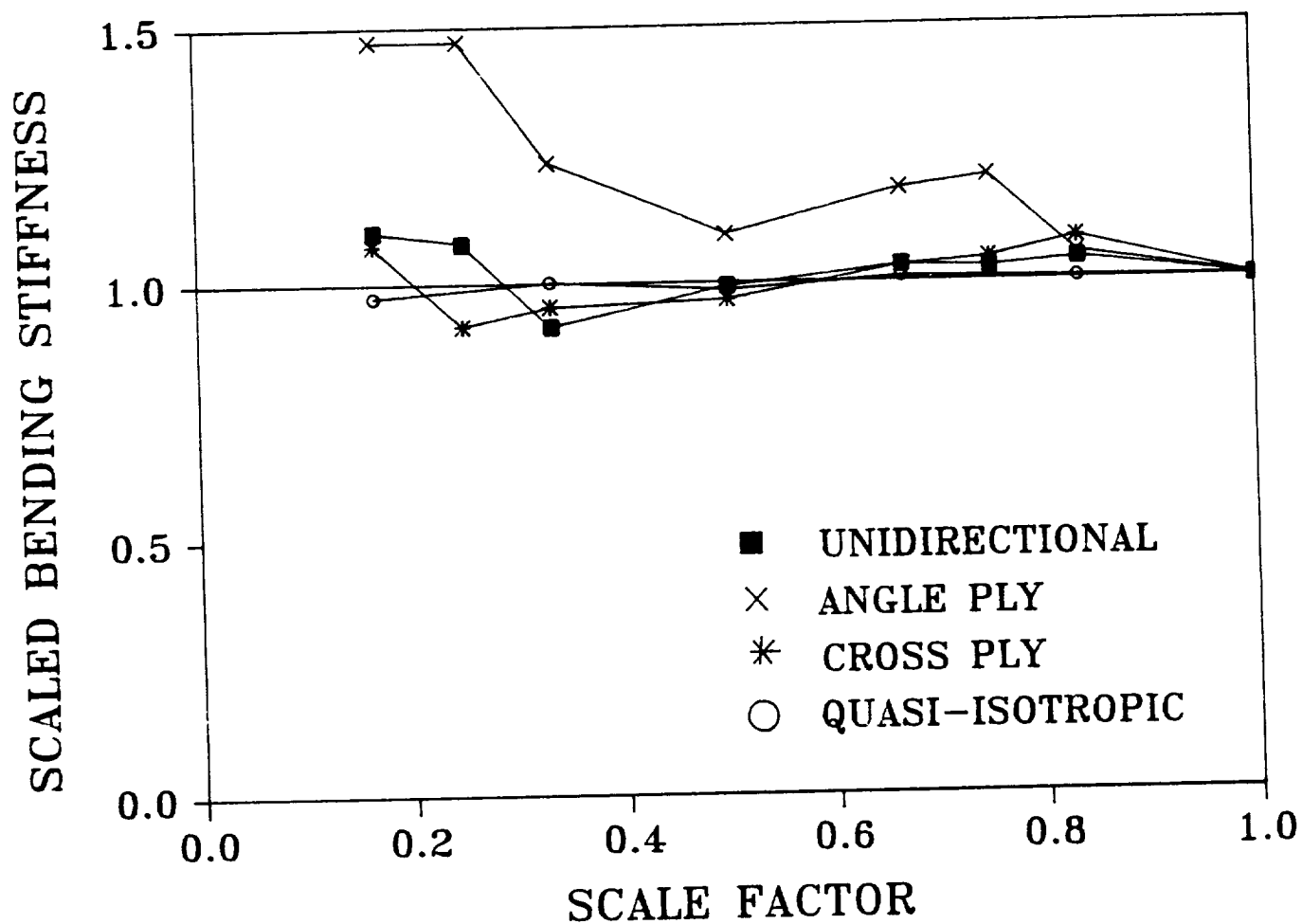


FIGURE 3. Normalized scaled bending stiffness versus scale factor for unidirectional, angle ply, cross ply, and quasi-isotropic beams loaded in flexure.

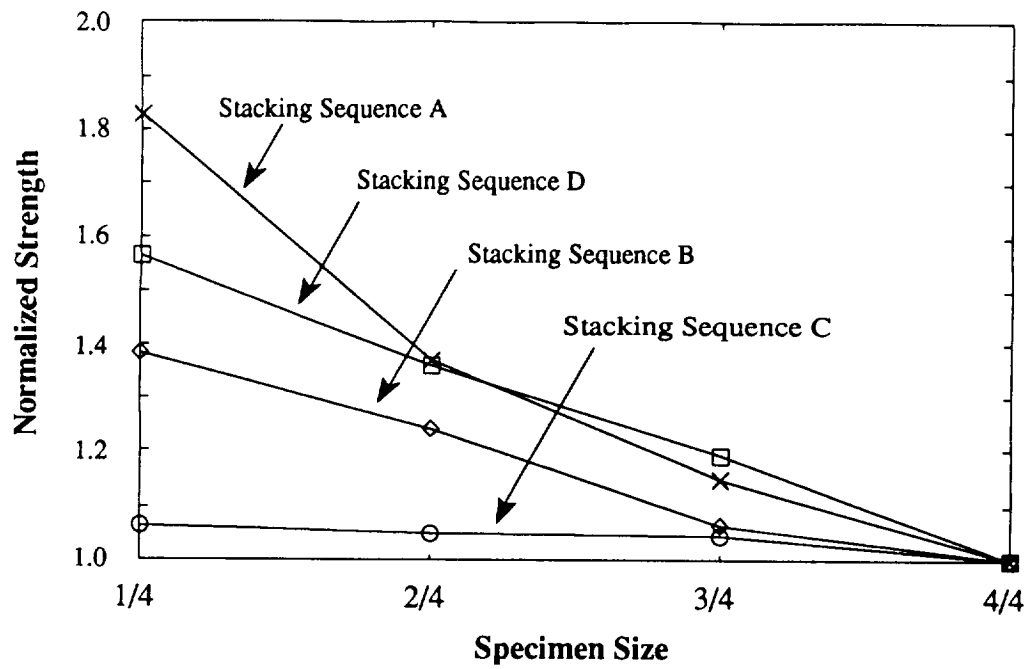


FIGURE 4. Normalized strength versus specimen size for Laminates A-D loaded in tension.

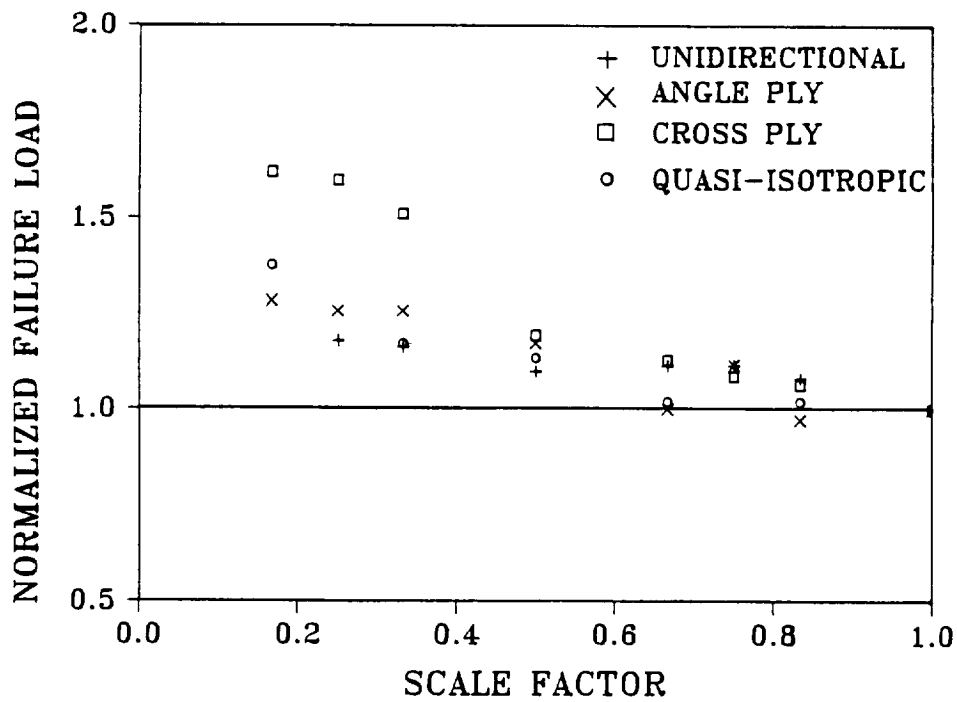


FIGURE 5. Normalized failure load versus scale factor for unidirectional, angle ply, cross ply, and quasi-isotropic beams tested under flexural loading.

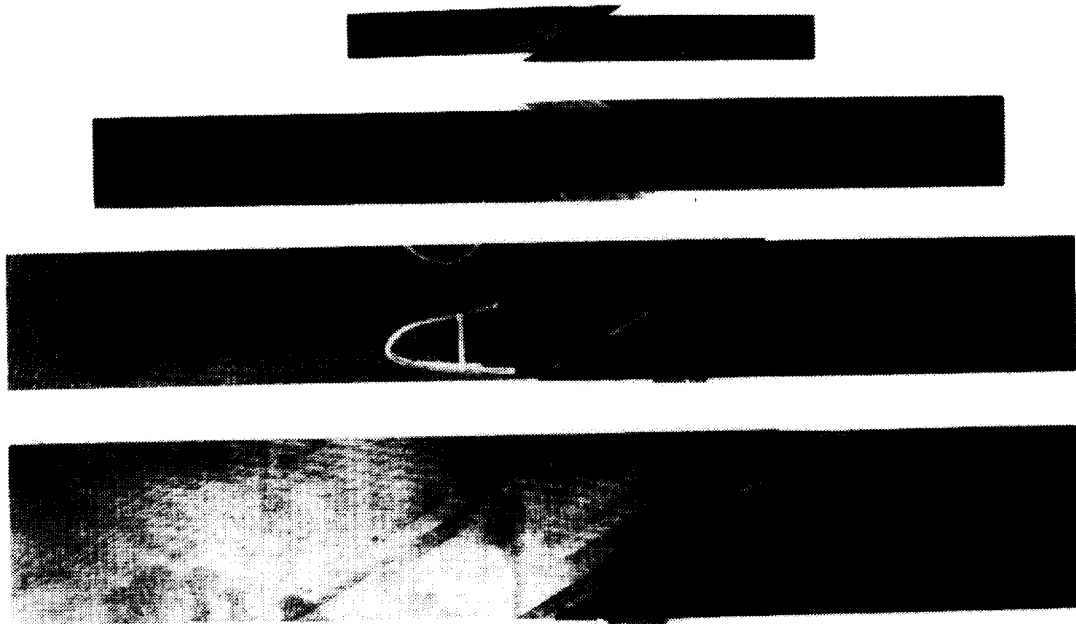


FIGURE 6. Typical failures in four scaled size specimens of Laminate A loaded in tension.

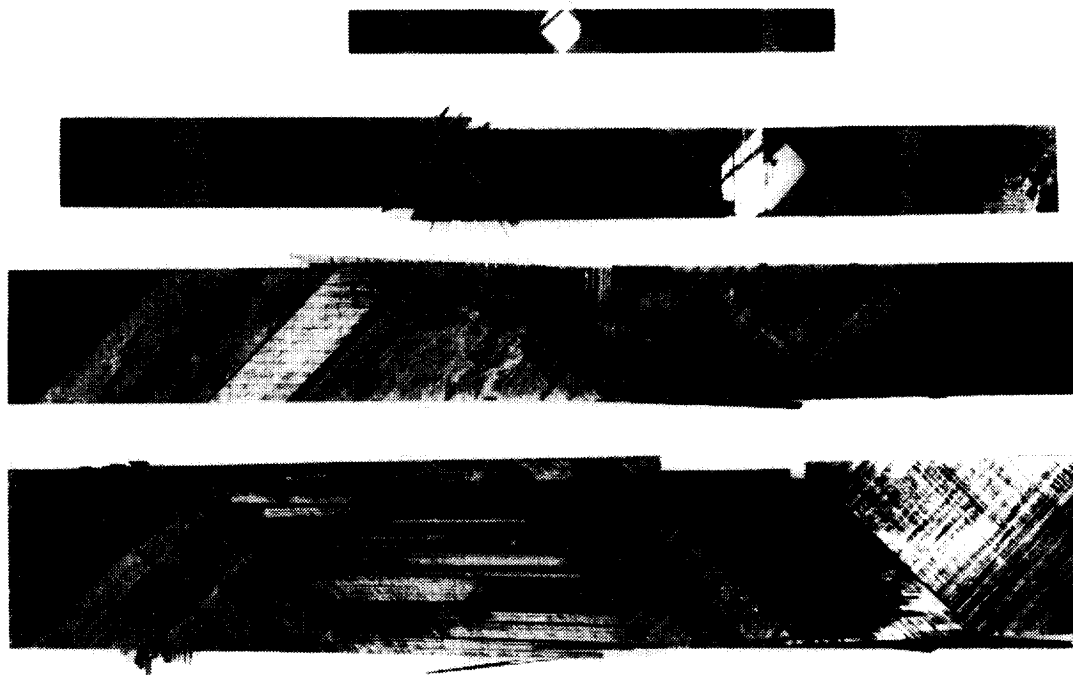


FIGURE 7. Typical failures in four scaled size specimens of Laminate B loaded in tension.

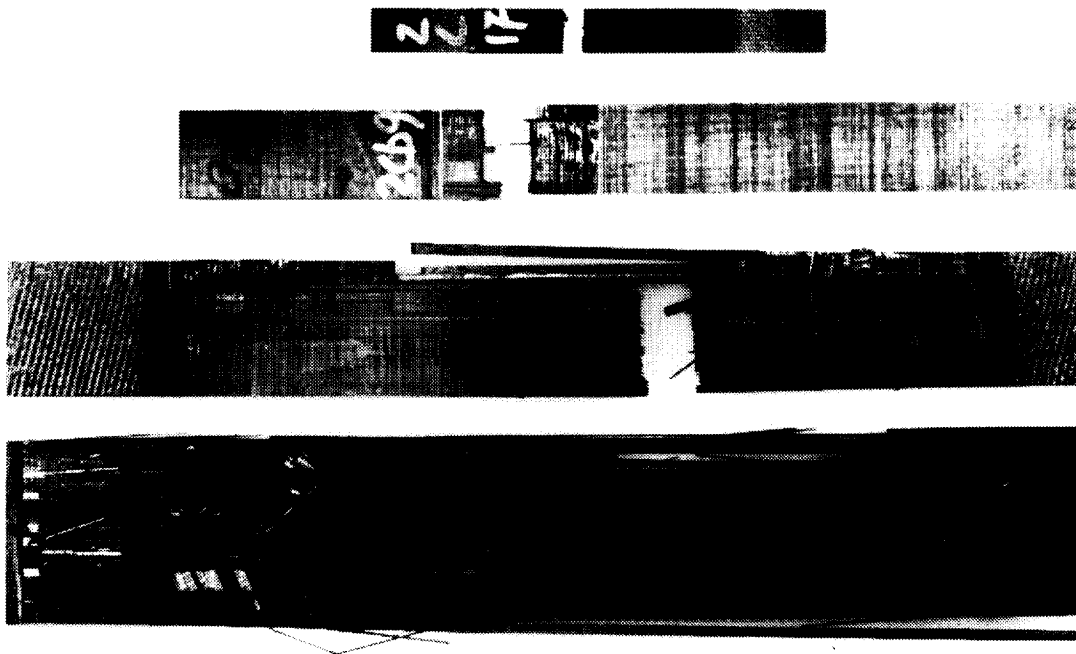


FIGURE 8. Typical failures in four scaled size specimens of Laminate C loaded in tension.

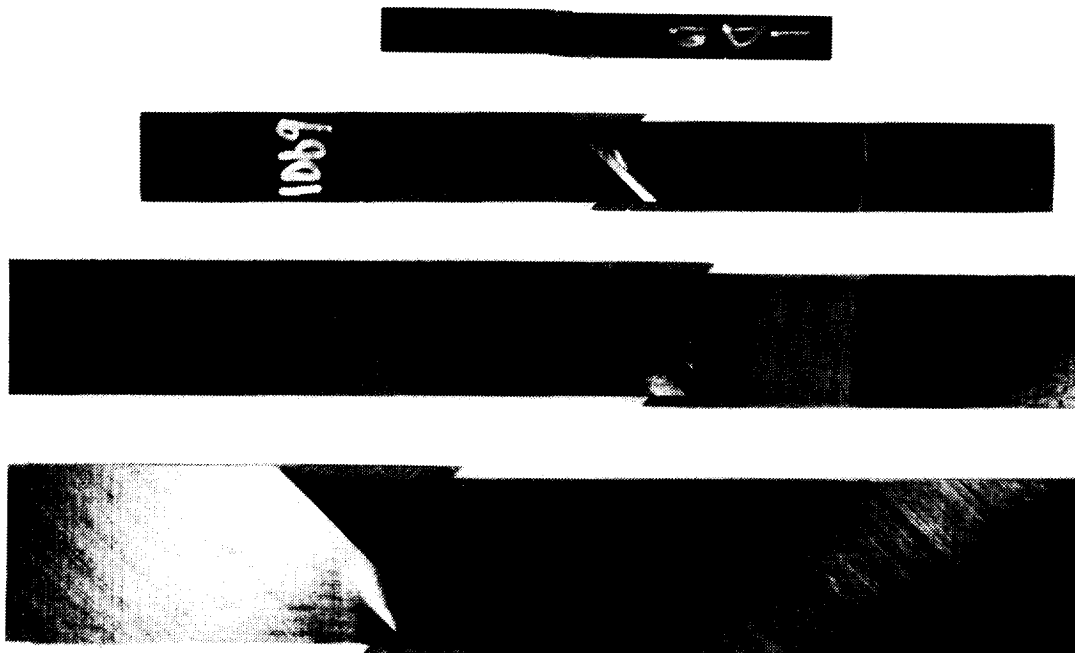


FIGURE 9. Typical failures in four scaled size specimens of Laminate D loaded in tension.

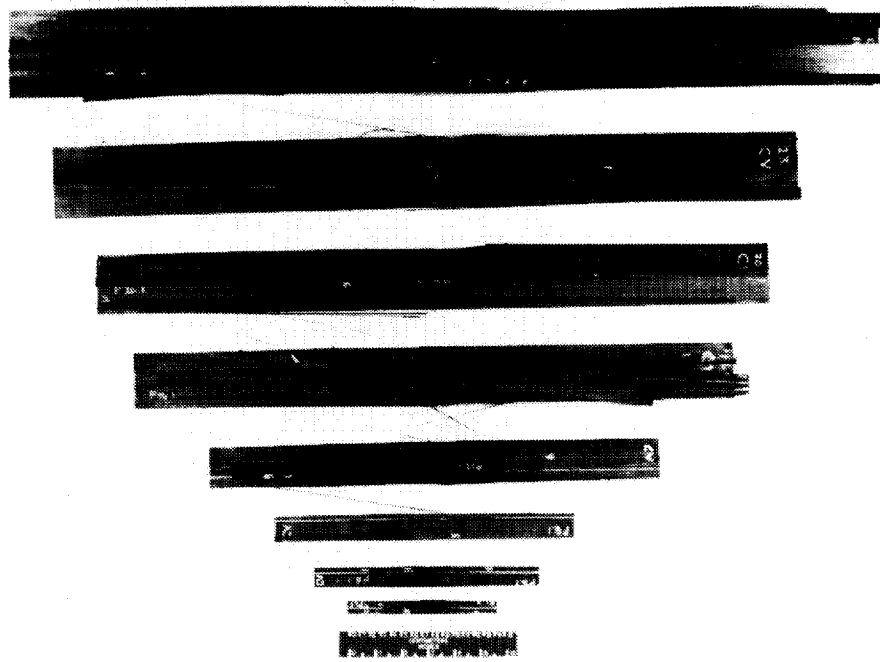


FIGURE 10. Failed unidirectional beams (1/6 through full-scale) tested under flexure.

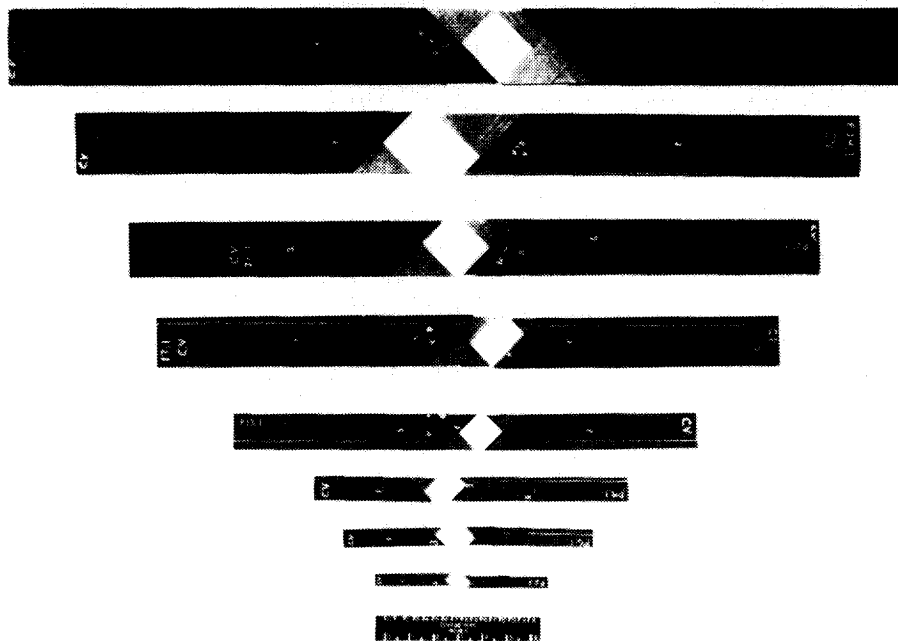


FIGURE 11. Failed angle ply beams (1/6 through full-scale) tested under flexure.



FIGURE 12. Failed cross ply beams (1/6 through full-scale) tested under flexure.

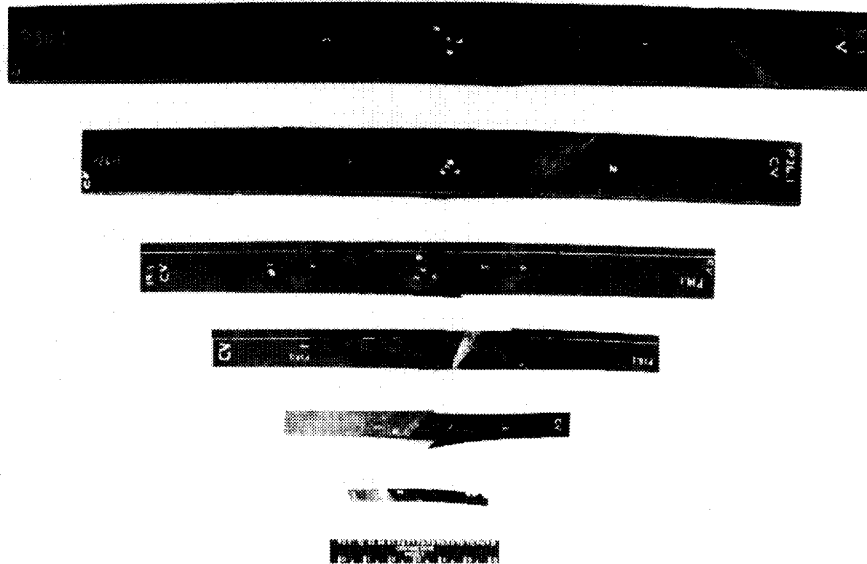


FIGURE 13. Failed quasi-isotropic ply beams (1/6 through full-scale) tested under flexure.

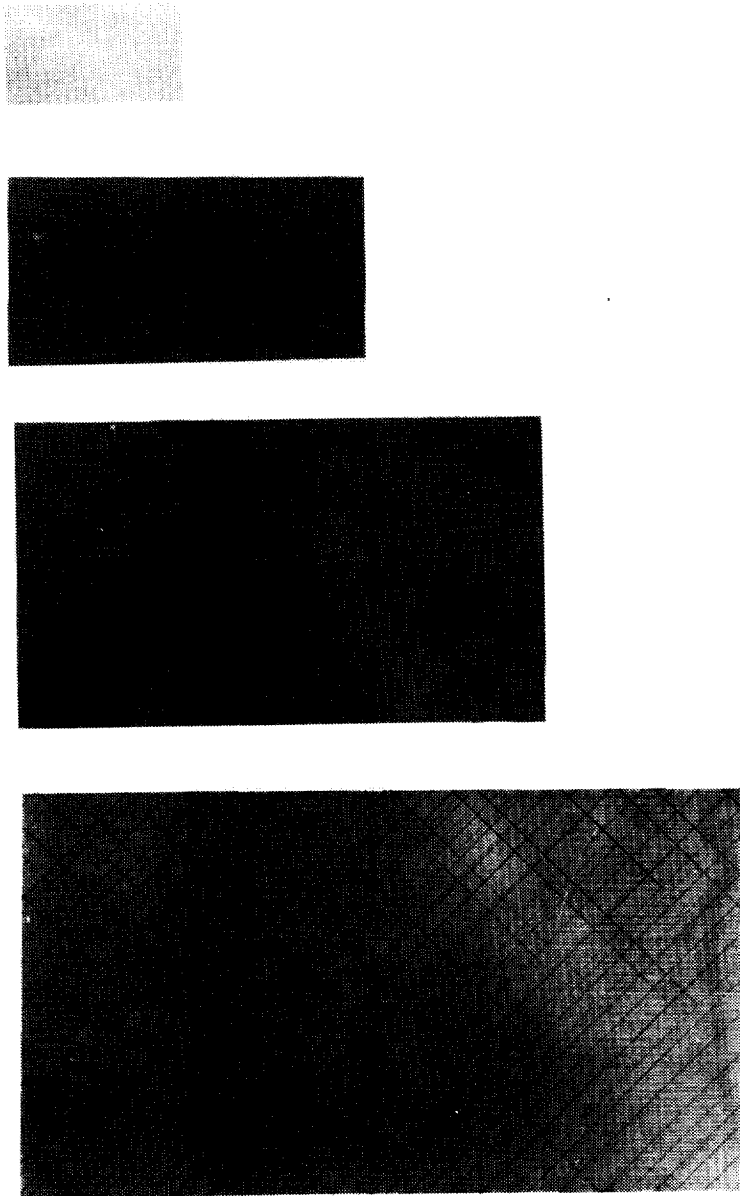


FIGURE 14. X-ray radiographs of virgin specimens of Laminate D.

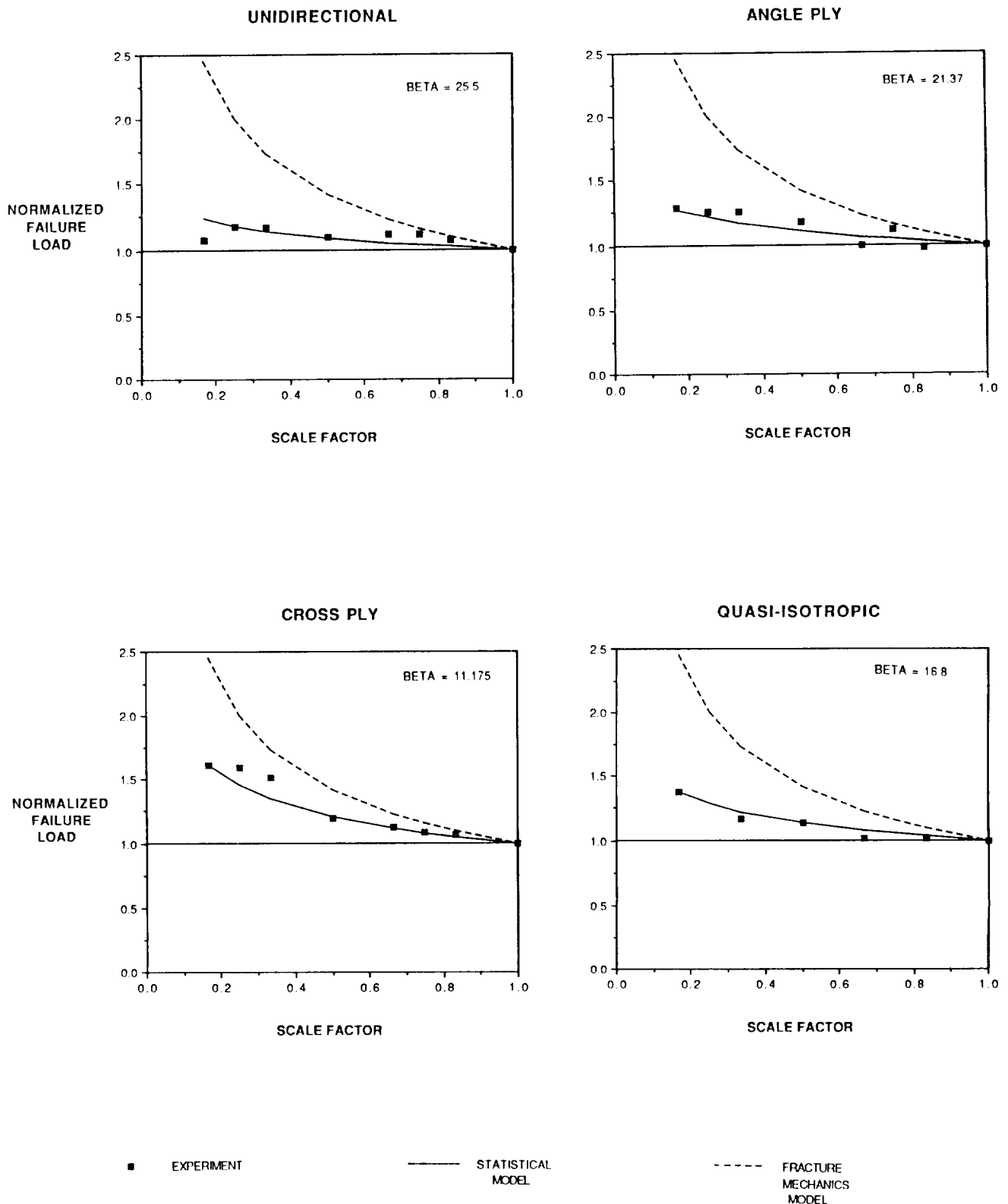


FIGURE 15. A comparison of normalized failure load versus scale factor with statistical and fracture mechanics based analytical models for unidirectional, angle ply, cross ply, and quasi-isotropic scale model beams tested under flexural loading.

